

# Undercover Deepfakes: Detecting Fake Segments in Videos

Sanjay Saha\*, Rashindrie Perera<sup>†§</sup>, Sachith Seneviratne<sup>†§</sup>, Tamasha Malepathirana<sup>†</sup>, Sanka Rasnayaka\*,  
Deshani Geethika<sup>†</sup>, Terence Sim\*, Saman Halgamuge<sup>†</sup>

\*National University of Singapore, Singapore

<sup>†</sup>University of Melbourne, Australia

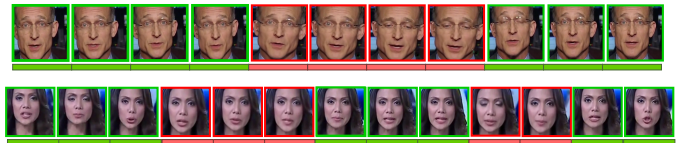
sanjaysaha@u.nus.edu\*, cdperera@student.unimelb.edu.au<sup>†</sup>, sachith.seneviratne@unimelb.edu.au<sup>†</sup>,  
tmalepathira@student.unimelb.edu.au<sup>†</sup>, sanka@nus.edu.sg\*, dpoddenige@student.unimelb.edu.au<sup>†</sup>,  
terence.sim@nus.edu.sg\*, saman@unimelb.edu.au<sup>†</sup>

**Abstract**—The recent renaissance in generative models, driven primarily by the advent of diffusion models and iterative improvement in GAN methods, has enabled many creative applications. However, each advancement is also accompanied by a rise in the potential for misuse. In the arena of deepfake generation this is a key societal issue. In particular, the ability to modify segments of videos using such generative techniques creates a new paradigm of deepfakes which are mostly real videos altered slightly to distort the truth. Current deepfake detection methods in the academic literature are not evaluated on this paradigm. In this paper, we present a deepfake detection method able to address this issue by performing both frame and video level deepfake prediction. To facilitate testing our method we create a new benchmark dataset where videos have both real and fake frame sequences. Our method utilizes the Vision Transformer, Scaling and Shifting[30] pretraining and Timeseries Transformer to temporally segment videos to help facilitate the interpretation of possible deepfakes. Extensive experiments on a variety of deepfake generation methods show excellent results on temporal segmentation and classical video level predictions as well. In particular, the paradigm we introduce will form a powerful tool for the moderation of deepfakes, where human oversight can be better targeted to the parts of videos suspected of being deepfakes. All experiments can be reproduced at: <https://github.com/sanjaysaha1311/temporal-deepfake-segmentation>.

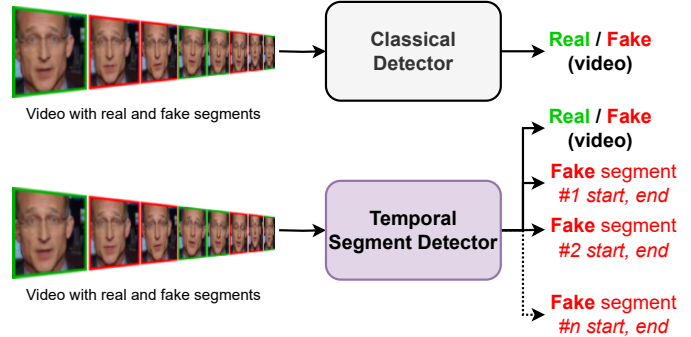
## I. INTRODUCTION

Deep learning has made significant advances over the last few years, with varying degrees of societal impact. The advent of diffusion models as viable alternatives to hitherto established generative models has revolutionized the domains of textual/language learning, visual generation, and cross-modal transformations [43]. This, alongside other recent advancements in generative AI such as GPT4 [4] has also brought to attention the social repercussions of advanced AI systems capable of realistic content generation.

There exist many methods to tackle the deepfake detection problem formulated as a binary classification problem[1], [3], [8]. A common pitfall of these methods is the inability to generalize to unseen deepfake creation methods. However, there is a more pressing drawback in these studies that we aim to highlight and address in this paper. Considering the



(a) Visualization of two sample videos in the newly introduced benchmark dataset for temporal deepfake segment detection.



(b) Comparison of our method with the classical deepfake detection.

Fig. 1: (a) We propose a new deepfake benchmark dataset consisting of videos with one or two manipulated segments, represented in the two images respectively. Fake frames are indicated by smaller red boxes and genuine video frames are denoted by green borders. (b) Our proposed deepfake detection method employs temporal segmentation to classify video frames as real or fake and identify the intervals containing the manipulated content. This is a departure from the conventional binary classification of videos as either entirely genuine or entirely manipulated.

social impact of a deepfake video, we hypothesize that rather than fabricating an entire fake video, a person with malicious intent would alter smaller portions of a video to misrepresent a person's views, ideology and public image. For example, an attacker can generate a few fake frames to replace some real frames in a political speech, thus distorting their political views which can lead to considerable controversy and infamy.

The task of identifying deepfake alterations within a longer video, known as deepfake video temporal segmentation, is

<sup>§</sup>Equal contribution

currently not well explored or understood. These types of deepfakes pose a more difficult challenge for automated deepfake analysis compared to other types of deepfakes. Moreover, they also pose a greater threat to society since the majority of the video may be legitimate, making it appear more realistic and convincing. Additionally, these deepfakes require significant manual oversight, especially in the moderation of online content platforms, as identifying the legitimacy of the entire video requires manual interpretation. However, performing frame-level detection allows the human moderator to save time by focusing only on the fake segments.

Figure 1(a) demonstrates deepfake videos where the entire video is not fake, but some of the real frames were replaced by fake frames. We present a benchmark dataset with videos similar to those in Figure 1(a) to test our method on the temporal deepfake segmentation problem. In the temporal deepfake segmentation problem the detector makes frame level predictions and calculates the start and end of the fake sequences. This differs from classical deepfake detection where the detector makes a video level prediction as demonstrated in Figure 1(b).

### Problem Definition

Deepfake Temporal Segmentation Task is defined as follows,

*Given an input video identify temporal segments within the video that are computer generated i.e. fakes.* The output of this task is a labeling of ‘real’ or ‘fake’ for each frame, which we call a temporal segmentation map. We can frame the classical deepfake detection problem as a special case of the temporal segmentation task, in which ALL frames are labeled either as ‘real’ or ‘fake’. With an emphasis on the novel deepfake temporal segmentation task, this paper makes the following contributions,

- We identified the new threat of faking small parts of a longer video to pass it off as real. Current detection methods cannot handle this threat, since they assume the entire video is real or fake. This can be addressed through our proposed temporal segmentation of videos. This novel problem provides a new direction for future research.
- We curated a new dataset specifically for deepfake temporal segmentation, which will be publicly available for researchers to evaluate their methods. Our rigorous experiments establish benchmark results for temporal segmentation of deepfakes, providing a baseline for future work.

## II. RELATED WORK

### A. Face Image Synthesis

Manipulation of face images has always been a popular research topic in the media forensics and biometrics domain. Synthesized digital faces can be used to deceive humans as well as machines and software. Prior to deepfakes, digitally manipulated faces[45], [46], [22] were utilized mainly to fool biometric verification and identification methods e.g., face recognition systems. Consequently, deepfake methods[19],

[11], [10], [56] started to generate very realistic fake videos of faces and became much more popular as a result. This led to a series of research works on developing a number of deepfake generation methods, categorized into mainly two types: Face swapping[12], [25], [38] and Face reenactment[50], [48].

Deepfake generation methods have since improved by a significant margin through the advancement of existing methods and better software integration as in Deepfacelab[38]. This has helped creators of deepfakes to create longer videos, including seamlessly blending fake frames with real frames which allows to have both real and fake video segments within a same deepfake video. Through more recent developments in generative AI[43], [51], [37] we are at the brink of experiencing even higher quality and more subtle deepfakes which raises the need for updated research in this area.

### B. Deepfake Detection

Initial works on deepfake detection methods focused on detecting artifacts in the deepfaked face images such as irregular eye colors, asymmetrically blinking eyes, abnormal heart beats, irregular lip, mouth and head movements[28], [47], [7], [34]. Some other earlier works tried to find higher level variability in the videos: erroneous blending after face swaps, or identity-aware detection approach[54], [15], [26], [9]. Compared to these earlier works more recent studies[36], [41], [2] that are independent of artifact based detection have achieved astounding results in detecting fake videos from most of the state-of-the-art datasets. Recently, more works[5], [53], [55], [20], [35], [23], [18], [17] have given more attention towards generalization of the detectors. Although deepfake detection methods have seen significant progress in recent years, most of the previous works have assumed that an entire video is fake even when only a short segment is altered while the rest of the frames are real. In contrast, in this paper, we introduce the concept of not only detecting deepfake videos but also segmenting the fake frames within them. The proposed approach can accurately identify one or more fake segments in a deepfake video which can mitigate the risks associated with deepfakes that incorporate only a few fake segments.

## III. METHODOLOGY

We propose a two-stage method, where, in the first stage we use a Vision Transformer (ViT) with Scaling and Shifting (SSF). With the learned frame-level features from the first stage, we train a Timeseries Transformer (TsT) which learns the temporal features and helps to segment deepfake videos temporally. The preprocessing is simple, it includes extraction of the frames and cropping of the face region. The ViT from the first stage of our method learns the spatial features through fine-tuning with the help of SSF. The ViT learns frame-level features which comprise a single vector for each frame. These features are the inputs to the TsT classifier (the second stage of our method). The TsT is an adaptation of the original transformer encoder from [52], it helps in learning temporal features from sequential data such as the learned ViT features and uses the temporal features for classification. The

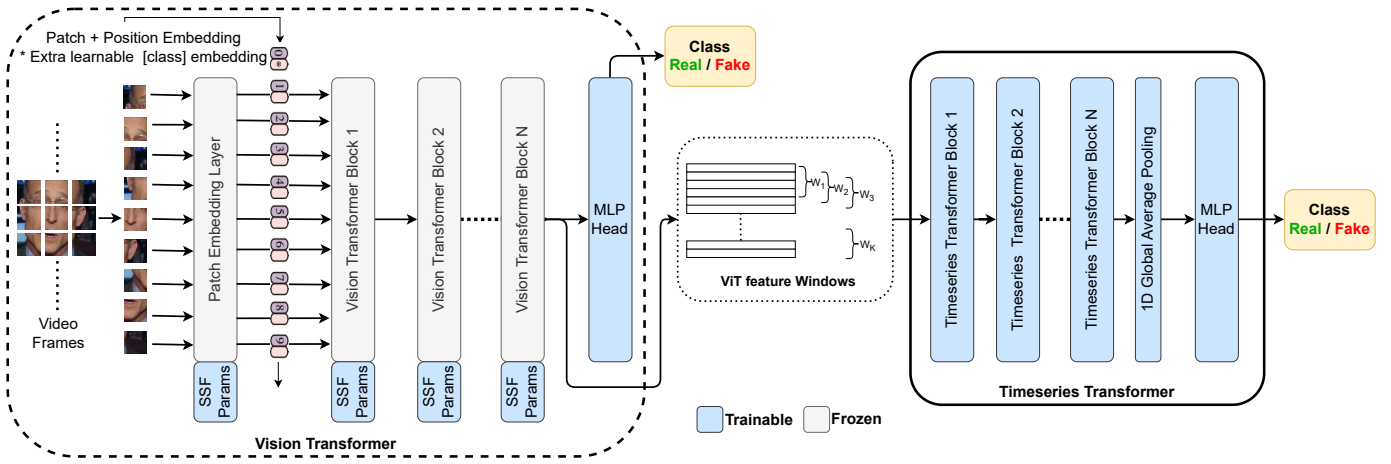


Fig. 2: Our proposed method’s model architecture comprises two main blocks: the Vision Transformer (ViT) and the Timeseries Transformer (TsT). The ViT fine-tunes a pre-trained model for deepfake detection using the Scaling and Shifting (SSF) method, learning spatial features. On the other hand, the TsT focuses on temporal features. The ViT’s spatial features are sequentially accumulated and split into overlapping windows before inputting into the TsT.

	Ratio of fake frames		Average Length
	One seg.	Two seg.	
Deepfakes (DF)	0.231	0.389	668.5
Face-Shifter (FSh)	0.231	0.389	668.5
Face2Face (F2F)	0.233	0.393	662.0
Neural Textures (NT)	0.264	0.444	585.3
FaceSwap (FS)	0.264	0.444	585.3
<b>Average</b>	<b>0.243</b>	<b>0.411</b>	<b>633.9</b>

TABLE I: Ratio of fake frames in the benchmark dataset. This benchmark dataset is based on FaceForensics++ (FF++) and has the same sub-datasets as FF++. The ratio of fake frames differs among sub-datasets due to the original fake videos having different number of total frames. Average length is calculated in terms of number of frames in a video. Each segment of fake frames is contiguous.

feature vectors from stage 1 are sequentially accumulated and windowed through sliding window technique. It is important to use sequentially windowed feature vectors as input to the TsT since we need the temporal features to be learned for better temporal segmentation.

### A. Model architecture

1) *Vision Transformer (ViT) and Scaling and Shifting (SSF)*: Vision transformers (ViT) have achieved state-of-the-art results on several image classification benchmarks, demonstrating their effectiveness as an alternative to convolutional neural networks (CNNs). The ViT model first partitions the input image  $I \in \mathbb{R}^{H \times W \times C}$  into a set of smaller patches of size  $N \times N$  where  $H$ ,  $W$ , and  $C$  correspond to the height, width, and the number of channels of the image respectively. Each patch is then represented by a  $d$ -dimensional feature vector, which is obtained by flattening the patch into a vector of size  $N^2C$  and applying a linear projection to reduce its dimensionality. Next, to allow the model to learn the spatial relationships between the patches, positional encodings are added to the patch

embeddings. The resulting patch embeddings are concatenated together to form a sequence, and a learnable class embedding that represents the classification output is prepended to the sequence which is then input through a series of transformer layers. Each transformer layer consists of a multi-head self-attention mechanism, which allows the model to attend to different parts of the input patches, a multi-layer perceptron, and a layer normalization (Fig. 2). Finally, a classification head is attached at the end of the transformer layers which produces a probability distribution over the target classes.

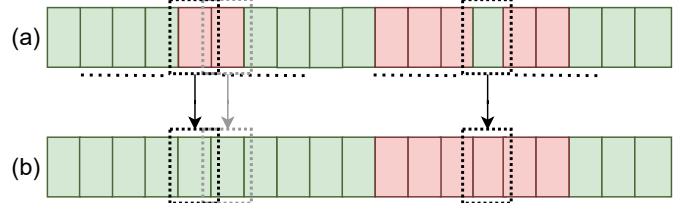


Fig. 3: This figure depicts the visualization of our proposed approach for smoothing out noisy predictions. The first image (a) illustrates the raw frame-level predictions for a video, while the second image (b) shows the output after applying Algorithm 1. Each small block in the images represents the model’s prediction for a frame, with green indicating ‘real’ and red indicating ‘fake’ prediction. The frames surrounded by dotted rectangles get their prediction changed based on the majority vote from past (left) and future (right) predictions, indicated by the dotted lines.

Recently, there has been an upsurge in the use of parameter-efficient fine-tuning methods[30], [6] to fine-tune only a smaller subset of parameters in large pre-trained models such as ViTs, leading to better performance in downstream tasks compared to conventional end-to-end fine-tuning and linear probing. We utilize one such method, called Scaling and

Shifting (SSF) [30] to train the ViT model used in our pipeline Fig. 2. SSF attempts to alleviate the distribution mismatch between the pre-trained task and the downstream deep fake feature extraction task by modulating deep features. Specifically, during the fine-tuning phase, the original network parameters are frozen, and scaling and shifting parameters are introduced at each operation to learn a linear transformation of features as shown in Fig. 2.

Formally, given the output from layer  $i$  as  $x \in \mathbb{R}^{N^2+1} \times d$ , the output  $y \in \mathbb{R}^{N^2+1} \times d$  (is also the input to the next operation) is calculated by

$$y = \gamma \cdot x + \beta \quad (1)$$

where  $\gamma \in \mathbb{R}^d$  and  $\beta \in \mathbb{R}^d$  are the scale and shift parameters, respectively. As done in the original work, we too insert SSF parameters after each operation with a linear coefficient in the ViT.

## 2) Timeseries Transformer: Architecture and training.

The timeseries transformer is an adaptation of the sequence to sequence transformer in [52]. The transformer architecture is designed to learn and classify from sequential data instead of generating another sequence. It is composed of multiple transformer blocks and an MLP (Multilayer Perceptron) head. Each transformer block has a multi-head attention mechanism and a feed forward block as shown in Figure 4(c).

Our method generates frame-level predictions for the input videos, which may contain some noisy predictions. To address this issue, we propose a simple smoothing technique (Figure 3) based on Algorithm 1. The algorithm sets a minimum duration for fake-segments, specified in terms of the number of frames. It processes each frame-prediction by computing the majority vote from past frames on the left and future frames on the right to determine the final label for that frame. By smoothing out the noisy predictions, our approach enhances performance, as demonstrated in Table V.

---

### Algorithm 1 Smoothing noisy predictions.

---

**Require:**  $\rho$ , the list of predictions per frame

**Require:**  $k \geq 0$ , the offset

```

for  $i \leftarrow 0 \dots \text{len}(\rho)$  do
   $\rho_{\text{left}} \leftarrow$  sub-list of size  $k$  on left of  $\rho[i]$ 
   $\rho_{\text{right}} \leftarrow$  sub-list of size  $k$  on right of  $\rho[i]$ 
   $M_{\text{left}} \leftarrow$  majority-vote( $\rho_{\text{left}}$ )
   $M_{\text{right}} \leftarrow$  majority-vote( $\rho_{\text{right}}$ )
  if  $\rho_{\text{left}}$  is empty and  $\rho[i] \neq M_{\text{right}}$  then
     $\rho[i] \leftarrow M_{\text{right}}$ 
  else if  $\rho_{\text{right}}$  is empty and  $\rho[i] \neq M_{\text{left}}$  then
     $\rho[i] \leftarrow M_{\text{left}}$ 
  else if  $M_{\text{left}} = M_{\text{right}}$  and  $\rho[i] \neq M_{\text{left}}$  then
     $\rho[i] \leftarrow M_{\text{left}}$ 
  end if
end for
return  $\rho$ 

```

---

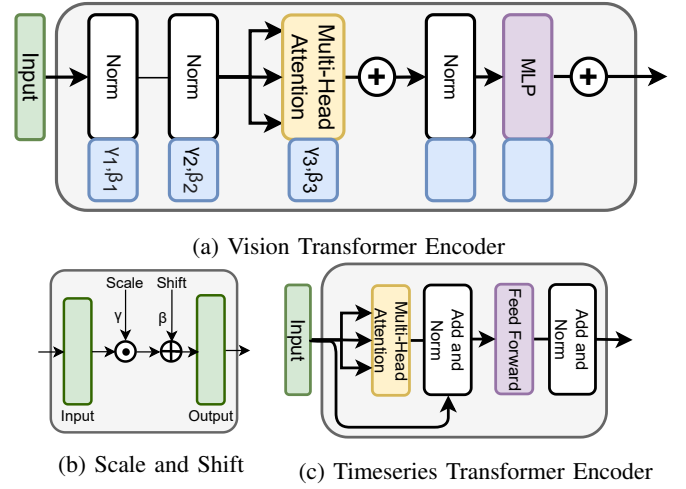


Fig. 4: Architecture of the encoder blocks and Scale and Shift block.

**Data processing.** The learned features from the vision transformer consists of a vector for each of the frames in the dataset. However, for the timeseries transformer we accumulated the frames sequentially for each video and split them into overlapping windows of size  $W$ . That is, we have features of  $W$  sequential frames in one window.

## B. Temporal Deepfake Segment Benchmark

Nearly all deepfake related studies have assumed that all the frames in a deepfake videos are from one class i.e. fake and real. However, it is possible to have both these types of frames within one video. With sophisticated deepfake generation methods such as Neural Textures[49], Deepfacelab[38] etc., it is possible to create fake segments that blend masterfully with the neighboring real segments within a video. This makes it very hard even for experienced human eyes to detect and to separate the fake segments from the real ones. Hence it is important to explore automated temporal segmentation of deepfake videos.

1) *Dataset:* The available deepfake datasets contain videos where all the frames in a video are from one class: ‘real’ or ‘fake’. To the best of our knowledge, there are no publicly available datasets which allow us to experiment with temporal segmentation. Therefore we created the first benchmark dataset with videos containing both fake and real frames to test temporal segmentation. The dataset was created from a re-sampled subset from the original FaceForensics++[44] (FF++) dataset. Since the distribution of any copy of the original dataset is limited, we will publish the code and necessary files to regenerate the temporal dataset instead of publishing the videos.

Each sub-dataset has 100 videos, totaling 500 videos with one fake segment, and 500 with two fake segments. It is important to note that FF++ dataset has five sub-datasets of fake videos and one set of real ones each containing 1000 videos. We have selected 100 videos with the same id across

the sub-datasets randomly with the condition that the length of the videos must be above 500 frames. For videos with one fake segment, we have selected a random starting point in the first half of the video and a random choice from 125, 150, and 175 frames for the length of the fake segment. The ratio of fake frames and the length of the videos for each deepfake generation method in the dataset are presented in Table I.

A similar strategy is selected for videos with two fake segments as well. In the case of two fake segments in a video, the first fake segment starts at a random position within the first 125 frames and the second fake segment starts at a random position within the first 75 frames in the second half of the video. The length of the fake segments here are randomly chosen as in the case of one segment videos. The information and code related to reproducing the dataset are published at: <https://github.com/sanjaysaha1311/temporal-deepfake-segmentation>.

2) *Evaluation: Intersection over Union (IoU)*: Intersection over Union (IoU) is proposed to evaluate the temporal segmentation map. This metric is most commonly used to evaluate the fit of object detection bounding boxes[42], [40]. 1-D variations of IoU has been adopted for time series segment analysis, which we will be utilizing.

Let the ground truth map be  $GT_{map}$  and predicted segmentation map be  $P_{map}$ . Both will be 1-D vectors of equal length with a predicted Boolean class ( $R$  or  $F$ ) for each frame in the video.

$$GT_{map} = \{RRRRRRFFFR... \} \quad (2)$$

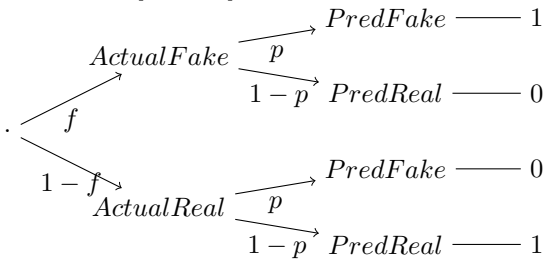
$$P_{map} = \{RRRRRRFFFR... \} \quad (3)$$

$$IoU = \frac{Intersection}{Union} = \frac{|GT_{map} \cap P_{map}|}{|GT_{map} \cup P_{map}|} \quad (4)$$

**Observation:**  $|GT_{map} \cap P_{map}|$  is the count of correctly predicted frames, and  $|GT_{map} \cup P_{map}|$  is the count of correctly predicted frames and wrongly predicted frames  $\times 2$ .

IoU falls in the range  $[0, 1]$ ; where the greater the value, the better the predicted segment map.

While the theoretical lower bound of IoU is zero, in practice it is useful to understand how a random guessing algorithm will be scored. Let  $f$  be the ratio of Real frames in the  $GT_{map}$  and  $p$  be the probability at which the randomly predicted frame in  $P_{map}$  is classified as Real. The graph below shows the possible  $|GT_{map} \cap P_{map}|$  values (call it  $S$ ).



For a single frame, the expected value of  $S$  is,

$$\begin{aligned} E(S) &= f.p.1 + f(1-p).0 + (1-f).p.0 + (1-f).(1-p).1 \\ &= 1 + 2.f.p - f - p = \alpha \end{aligned} \quad (5)$$

For  $T$  total frames  $E(S) = T\alpha$ . Using our observation above  $|GT_{map} \cup P_{map}| = 2(T - T\alpha)$ . Therefore IoU can be calculated as,

$$\begin{aligned} E(S) &= \frac{T\alpha}{T(2-\alpha)} \\ &= \frac{1 + 2.f.p - f - p}{1 - 2.f.p + f + p} \end{aligned} \quad (6)$$

For a random guessing algorithm with  $p = 0.5$  we have  $IoU = 1/3$  from equation (5). This will be the random guessing baseline for IoU in our context.

## IV. RESULTS

### A. Experimental settings

**Dataset.** Based on the recent deepfake detection methods we have used the FaceForensics++[44] (FF++) for training our models. There are five sub-datasets within FF++ and each sub-dataset has 1,000 videos in total. These five sub-datasets are prepared based on five different deepfake generation methods: Deepfakes (DF) [12], FaceShifter (FSh) [25], Face2Face (F2F) [50], NeuralTextures (NT) [48], FaceSwap (FS) [24]. Among the 1,000 in each sub-dataset we have used 800 for training and validation, and we tested on the remaining 200. We have experimented with the videos with compression level ‘c23’ and all the frames were used in the training and testing i.e. no frames were skipped.

To evaluate the temporal segmentation performance we have used our proposed novel benchmark dataset (see section III-B) for testing the temporal segmentation performance. This dataset is generated based on the original FF++ dataset, where each video contains both real and fake segments. There are 5 sub-datasets within the temporal dataset, same as the original FF++, each having 100 videos with an average of 633.9 frames per video, 24.3% fake frames for videos with one fake segment and 41.1% fake frames for videos with two fake segments. We also experimented on the other popular datasets: FF++, CelebDF[29], DFDC[13] and WildDeepFakes[57]. These datasets were used to compare our method’s performance in terms of traditional deepfake detection experiments: classical (same-dataset) deepfake detection and generalizability (cross-dataset).

For face extraction and alignment we have used DLIB[21], and the aligned face images were resized to  $224 \times 224$  for all the frames in train and test sets.

**Settings. Vision Transformer (ViT) and Shift and Scaling (SSF).** We use the ViT-B/16[14] architecture as the backbone for our ViT model and trained it using four A100 GPUs with a batch size of 64 for 80 epochs. The optimization algorithm used was ‘AdamW’ with a weight decay of 0.05. A warm-up strategy was applied for the learning rate, starting with  $1e^{-7}$  for the first five epochs and then increasing linearly to  $1e^{-3}$ . The dropout probability was set to 0.1, and the input image size was set to  $224 \times 224$ . To improve performance, a model exponential moving average was used

	DF				FSh				F2F				NT				FS				FF++			
	One seg		Two seg		One seg		Two seg		One seg		Two seg		One seg		Two seg		One seg		Two seg		One seg		Two seg	
	IoU	AUC	IoU	AUC	IoU	AUC	IoU	AUC	IoU	AUC	IoU	AUC	IoU	AUC	IoU	AUC	IoU	AUC	IoU	AUC	IoU	AUC	IoU	AUC
<b>DF</b>	<b>0.987</b>	<i>0.986</i>	<b>0.975</b>	<b>0.984</b>	0.926	0.917	0.886	0.923	0.963	0.96	0.937	0.959	0.748	0.729	0.603	0.723	0.954	0.956	0.920	0.954	0.915	0.912	0.860	0.910
<b>FSh</b>	0.957	0.963	0.933	0.958	<i>0.972</i>	<i>0.984</i>	<i>0.961</i>	<i>0.980</i>	0.971	0.969	0.947	0.966	0.764	0.748	0.628	0.745	0.966	0.968	0.938	0.965	0.926	0.928	0.878	0.924
<b>F2F</b>	0.970	0.976	0.959	0.976	0.971	0.978	0.954	0.972	<b>0.982</b>	<i>0.986</i>	<b>0.974</b>	<b>0.984</b>	0.840	0.836	0.739	0.832	<b>0.983</b>	0.985	<i>0.966</i>	<i>0.981</i>	0.950	0.953	0.918	0.950
<b>NT</b>	0.971	0.985	0.961	0.980	0.969	0.983	0.958	0.979	0.963	0.980	0.955	0.977	<i>0.949</i>	<b>0.974</b>	<i>0.933</i>	<i>0.966</i>	0.946	0.970	0.932	0.965	<i>0.960</i>	<i>0.979</i>	<i>0.949</i>	<i>0.974</i>
<b>FS</b>	0.941	0.935	0.898	0.932	0.963	0.962	0.931	0.955	0.970	0.970	0.950	0.969	0.679	0.679	0.514	0.642	<i>0.981</i>	<i>0.987</i>	<b>0.967</b>	<b>0.983</b>	0.904	0.901	0.842	0.898
<b>FF++</b>	<i>0.974</i>	<b>0.988</b>	<i>0.962</i>	<i>0.982</i>	<b>0.974</b>	<b>0.989</b>	<b>0.962</b>	<b>0.982</b>	<i>0.975</i>	<b>0.988</b>	<i>0.965</i>	<i>0.983</i>	<b>0.959</b>	<i>0.972</i>	<b>0.938</b>	<b>0.967</b>	0.975	<b>0.988</b>	0.955	0.978	<b>0.971</b>	<b>0.985</b>	<b>0.957</b>	<b>0.979</b>

TABLE II: Results for temporal segmentation on the proposed benchmark temporal deepfake dataset. Each row indicates a model trained on a specific training sub-dataset; we have trained models with FaceForensics++ (FF++) and the five sub-datasets within FF++ i.e. Deepfakes (DF), Face-Shifter (FSh), Face2Face (F2F), Neural Textures (NT) and FaceSwap (FS). The last row presents the results for the model trained on the full FF++ dataset. The columns represent the data we have tested our models on; similar to training we have tested the models on all the five sub-datasets of FF++ and the whole FF++ (i.e. last four columns). For each test data, we used the one-fake-segment and two-fake-segments test data from our proposed benchmark dataset (see section III-B). We report IoU and AUC metrics with the best value in a column is in **bold** and the second-best is in *italic*.

with a decay rate of 0.99992 together with automatic mixed precision. The model was initialized with pretrained weights on Imagenet-21K-SSF.

**Timeseries settings.** The dimension of the feature vector for each frame from the ViT was 768. After widening these vectors as shown in Figure 2 the input dimension for the Timeseries Transformer (TsT) was  $(W, 768)$ . In our experiments, we used  $W = 5$  however it is also possible to use different values for  $W$ . There are a total of 8 transformer blocks in the TsT, with 8-headed attention connection. Each attention-head’s dimension is 512. After the transformer blocks, we have 1-dimensional global average pooling prior to the MLP head. We have used categorical cross-entropy as the loss and ‘Adam’ as the optimizer with  $1e^{-4}$  learning for training this model. We used an early stopping technique with patience 10 to make the training procedure faster, training the TsT for 16 epochs with a batch size of 64.

### B. Temporal segmentation analysis

We have used our proposed benchmark dataset to test our method for the temporal segmentation problem where we try to classify deepfake videos in frame-level instead of video-level. The metrics we use to measure the performance for temporal segmentation are Intersection over Union (IoU) and Area under the ROC Curve (AUC). The baseline IoU (for random guessing the class of a frame) is  $1/3$  as shown in section III-B2. We have trained six separate models on six training sets: FaceForensics++ (FF++) and the five sub-datasets within FF++ i.e. Deepfakes (DF), Face-Shifter (FSh), Face2Face (F2F), Neural Textures (NT) and FaceSwap (FS). Similarly, we report the results for each model on the six test sets (FF++ and its five sub-datasets) in Table II.

As seen, each model does very well when it was tested on the test-set from the same dataset as it was trained on, hence the results on the diagonals are either the best or the second-best in every column while the second-best results are

	DF	FSh	F2F	NT	FS	FF++	C-DF	DFDC	WDF
<b>DF</b>	<b>0.993</b>	0.965	0.975	0.830	0.967	0.946	0.590	0.558	0.631
<b>FSh</b>	0.980	<i>0.990</i>	0.978	0.848	0.980	0.955	0.609	0.535	0.619
<b>F2F</b>	<i>0.990</i>	<b>0.993</b>	<b>0.990</b>	0.917	<i>0.993</i>	<i>0.977</i>	0.670	0.603	0.676
<b>NT</b>	0.973	0.967	0.967	<i>0.965</i>	0.960	0.967	<i>0.715</i>	<i>0.626</i>	<i>0.693</i>
<b>FS</b>	0.960	0.975	0.982	0.770	<b>0.995</b>	0.936	0.584	0.512	0.611
<b>FF++</b>	0.985	0.983	<i>0.983</i>	<b>0.967</b>	0.983	<b>0.982</b>	<b>0.790</b>	<b>0.667</b>	<b>0.703</b>

TABLE III: Results (in AUC) for video level classification. Similar to Table II each row represent results from models trained on specific training data. The columns constitute the test data. Along with FF++ and the sub-datasets of FF++ we have tested each model on other datasets such as CelebDF (C-DF), DFDC, and WildDeepFakes (WDF). The best value in a column is in **bold** and the second-best is in *italic*.

only lower in the range from 0.001 to 0.009. As expected, the model trained on the whole FF++ is the overall best-performing model.

However, the results from the other five models give us some important findings. Out of the five sub-datasets in FF++, three were made with a face swapping technique (DF, FSh and FS) and the other two were made with face re-enactment (F2F and NT). We can notice that models trained on F2F and NT perform better than the other three models. Since face re-enactment deepfakes are devoid of strong artifacts compared to face swapping deepfakes, models trained on face re-enactment methods tend to generalize well to other methods. Similarly, models trained on the face swapping methods do not generalize well to face re-enactment test data as seen on the ‘F2F’ and ‘NT’ columns in Table II. Overall, out of the five sub-datasets of FF++, NT is the best one to train a detection model if others are unavailable.



Method	CelebDF	FF++
Xception[44]	0.653	0.997
Face X-ray[26]	0.660	0.985
F3Net[39]	0.661	0.893
SMIL[27]	0.563	0.932
Two-branch[33]	0.734	0.932
SRM[32]	0.659	0.969
SPSL[31]	0.724	0.969
MADD[55]	0.674	<b>0.998</b>
SLADD[5]	<b>0.797</b>	0.984
Ours	0.790	0.982

TABLE IV: Comparison with other state-of-the-art methods in terms of AUC. The models were trained on FF++ and were evaluated on CelebDF and FF++. This comparison is for the video-level classification only, since existing works do not perform temporal segmentation. Most results from other methods were taken from their own paper and the rest were taken from [5]. Our method achieves competitive performance with state-of-the-art methods on generalizable deepfake detection.

### C. Video-level classification and Generalizability

The classical approach to deepfake detection has always been to predict the class (real or fake) of a deepfake video i.e. to make video-level predictions. We run experiments on the test data from the original datasets and report the results in Table III using AUC as the metric. We also measure our models’ performance on test data from datasets outside of FF++: CelebDF (C-DF), DFDC, and WildDeepFakes (WDF). Results for the sub-datasets of FF++ (DF, FSh, F2F, NT and FS) follow the results of the temporal analysis where the diagonal values are the best or the second-best in a column i.e. models when tested on data from the same sub-dataset generally perform very well. And, similar to the previous results (i.e. temporal segmentation) we see that models trained on face re-enactment data (F2F and NT) perform better than other sub-dataset-models when tested on unseen data i.e. these two models generalize well in comparison with other models. However, we see the best results from tests on CelebDF, DFDC, and WildDeepFakes from the model trained on the full FF++ dataset.

It is also noticeable that AUC scores for DFDC and Wild-DeepFakes are lower compared to CelebDF. While CelebDF is a dataset with videos made solely by the face swapping technique, DFDC is a combination of multiple methods such as face swapping (Deepfake Autoencoder and Morphable-mask), Neural talking-heads and GAN-based methods. Wild-DeepFakes dataset contains videos from the Internet which may contain videos generated using a variety of methods. Some of these methods are totally unseen due to their absence in the FF++ dataset.

We further evaluate and compare our results with state-of-the-art methods in Table IV using the model trained on FF++ and tested on FF++ and CelebDF. Our method performs

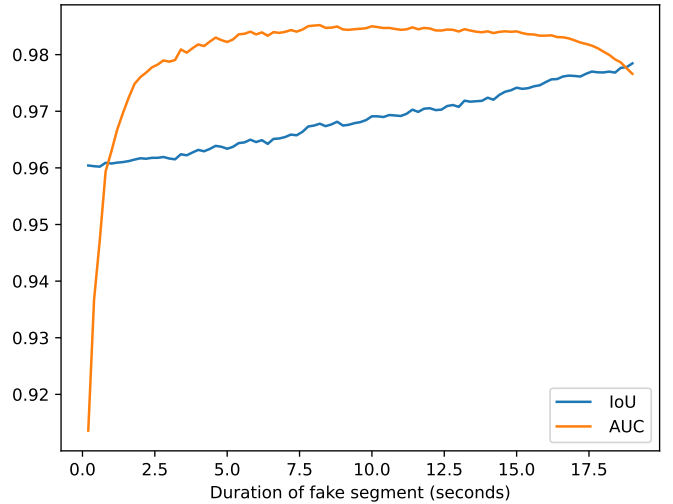


Fig. 5: Performance (IoU and AUC) of the proposed approach across different lengths of deepfake segments. Our approach is largely robust to variation in the length of the injected deepfake segment.

very competitively with the most recent state-of-the-art deepfake detection methods[5], [55] and outperforms most of the methods on the video-level predictions in both same-dataset and cross-dataset scenarios. Our method comprehensively exceeds the performance of several state-of-the-art methods such as Xception[44], F3Net[39], SMIL[27], Two-branch[33], SRM[32], SPSL[31] and MADD[55] in generalizability (i.e. cross-dataset/CelebDF). Also, our method does competitively well for the FF++ data while falling slightly behind only after Xception[44], MADD[55] and SLADD[5] by 0.016, 0.015 and 0.002 respectively. These results demonstrate that our method can also be used with high confidence for traditional deepfake detection and for unseen data (i.e. video-level) alongside temporal segmentation despite not being optimized for this objective.

### D. Varying Lengths of Fake Segments

Our proposed method is effective in identifying even short segments of deepfake that can significantly alter the message conveyed by a video. To evaluate the performance of our method, we conducted experiments on a test set comprising 100 videos with varying lengths of fake segments, and the results are presented in Figure 5. Specifically, we created fake segments with durations ranging from 0.2 seconds to 19 seconds, with an increment of 0.2 seconds, and calculated the average IoU and AUC over the 100 videos. The increment of 0.2 seconds is the average duration of two phonemes in English[16], which we assume to be the unit duration for a fake segment. Notably, we did not use the smoothing of noisy frames (Algorithm 1) in this experiment.

Our method achieves high accuracy in detecting very short fake-segments with a duration of less than 1.0 second, yielding an AUC value of over 0.91. Moreover, as the length of the fake

	Temporal Evaluation (IoU)			Video level (AUC)	
	ViT	ViT+TsT	ViT+TsT+Algo 1	ViT	ViT+TsT
<b>DF</b>	0.960	0.967 ( <b>+0.007</b> )	0.974 ( <b>+0.014</b> )	0.973	0.985 ( <b>+0.012</b> )
<b>FSh</b>	0.960	0.967 ( <b>+0.007</b> )	0.974 ( <b>+0.014</b> )	0.973	0.983 ( <b>+0.010</b> )
<b>F2F</b>	0.956	0.968 ( <b>+0.012</b> )	0.975 ( <b>+0.019</b> )	0.973	0.983 ( <b>+0.010</b> )
<b>NT</b>	0.933	0.948 ( <b>+0.015</b> )	0.959 ( <b>+0.026</b> )	0.965	0.967 ( <b>+0.002</b> )
<b>FS</b>	0.951	0.965 ( <b>+0.014</b> )	0.975 ( <b>+0.024</b> )	0.973	0.983 ( <b>+0.010</b> )
<b>FF++</b>	0.952	0.964 ( <b>+0.012</b> )	0.971 ( <b>+0.019</b> )	0.971	0.982 ( <b>+0.011</b> )

TABLE V: Ablation study on temporal segmentation of deepfakes and video-level classification. For temporal evaluation, results (IoU) from three experiments are reported: from Vision Transformer (ViT) only, with Timeseries Transformer (TsT) and also including Algorithm 1. Video level evaluation (in AUC) is reported for ViT, and ViT with TsT. Changes in the results are reported bold and are in brackets.

segment increases, our method performs even better in terms of both AUC and IoU. This experiment provides evidence that our proposed method can identify even the slightest alterations in very short fake-segments, highlighting its effectiveness in detecting deepfake videos.

#### E. Ablation study

We conducted experiments to evaluate the effectiveness of our proposed method without the TsT and the smoothing algorithm (Algorithm 1) for both the temporal segmentation detection and the video-level detection. The model was trained on the full FF++ training data and tested on the proposed temporal segmentation benchmark dataset and FF++ test set for temporal segmentation and video-level detection respectively. We used a MLP head on the ViT to classify frames for the experiment where the TsT was not included. Our ablated model achieved great results on both test sets, which are reported in Table V. To provide a better comparison, we also reported the results from the full model with the TsT and smoothing algorithm. While we observe that the ViT already performs very well, a significant improvement can be seen in both temporal and video-level performance with the inclusion of the TsT and the smoothing algorithm.

### V. DISCUSSION

While many methods tackle deepfake detection at the video-level, we propose a method that can generate results at the frame, segment and entire video level. This allows for maximal flexibility in analysing content for the presence of deepfakes and additionally provides comparison points for future research along these related but separate evaluation protocols.

Our method is based on supervised pretraining of the image encoder, which limits computational requirements in two forms. Firstly, the image encoder is trained independently on individual video frames with frame level supervision, nullifying the need for learning temporal relationships between frames. Secondly, a large part of the backbone is frozen and initialized using readily available weights from ImageNet, considerably reducing the computational cost of obtaining a

deepfake related representation in the encoder. The proposed method achieves robust IoU metrics across the proposed single and multi-segment analysis of deepfakes, while maintaining competitive performance on video-level deepfake detection and generalized deepfake detection.

### REFERENCES

- [1] D. Afchar, V. Nozick, J. Yamagishi, and I. Echizen. Mesonet: a compact facial video forgery detection network. In *2018 IEEE international workshop on information forensics and security (WIFS)*, pages 1–7. IEEE, 2018. 1
- [2] I. Amerini, L. Galteri, R. Caldelli, and A. Del Bimbo. Deepfake video detection through optical flow based cnn. In *Proceedings of the IEEE/CVF international conference on computer vision workshops*, pages 0–0, 2019. 2
- [3] B. Bayar and M. C. Stamm. A deep learning approach to universal image manipulation detection using a new convolutional layer. In *Proceedings of the 4th ACM workshop on information hiding and multimedia security*, pages 5–10, 2016. 1
- [4] S. Bubeck, V. Chandrasekaran, R. Eldan, J. Gehrke, E. Horvitz, E. Kamar, P. Lee, Y. T. Lee, Y. Li, S. Lundberg, et al. Sparks of artificial general intelligence: Early experiments with gpt-4. *arXiv preprint arXiv:2303.12712*, 2023. 1
- [5] L. Chen, Y. Zhang, Y. Song, L. Liu, and J. Wang. Self-supervised learning of adversarial example: Towards good generalizations for deepfake detection. In *Proceedings of the IEEE/CVF conference on computer vision and pattern recognition*, pages 18710–18719, 2022. 2, 7
- [6] S. Chen, C. Ge, Z. Tong, J. Wang, Y. Song, J. Wang, and P. Luo. Adapterformer: Adapting vision transformers for scalable visual recognition. *arXiv preprint arXiv:2205.13535*, 2022. 3
- [7] U. A. Ciftci, I. Demir, and L. Yin. Fakecatcher: Detection of synthetic portrait videos using biological signals. *IEEE transactions on pattern analysis and machine intelligence*, 2020. 2
- [8] D. Cozzolino, G. Poggi, and L. Verdoliva. Recasting residual-based local descriptors as convolutional neural networks: an application to image forgery detection. In *Proceedings of the 5th ACM workshop on information hiding and multimedia security*, pages 159–164, 2017. 1
- [9] D. Cozzolino, A. Rössler, J. Thies, M. Nießner, and L. Verdoliva. Id-reveal: Identity-aware deepfake video detection. In *Proceedings of the IEEE/CVF International Conference on Computer Vision*, pages 15108–15117, 2021. 2
- [10] F.-G. developer. Faceswap-gan. <https://github.com/shaoanlu/faceswap-GAN>. Accessed: 2023-02-16. 2
- [11] D. Developers. Dfaker. <https://github.com/dfaker/df>. Accessed: 2023-02-16. 2
- [12] D. F. Developers. Deepfakes. <https://github.com/deepfakes/faceswap>. Accessed: 2023-02-16. 2, 5
- [13] B. Dolhansky, J. Bitton, B. Pflaum, J. Lu, R. Howes, M. Wang, and C. C. Ferrer. The deepfake detection challenge (dfdc) dataset. *arXiv preprint arXiv:2006.07397*, 2020. 5
- [14] A. Dosovitskiy, L. Beyer, A. Kolesnikov, D. Weissenborn, X. Zhai, T. Unterthiner, M. Dehghani, M. Minderer, G. Heigold, S. Gelly, et al. An image is worth 16x16 words: Transformers for image recognition at scale. *arXiv preprint arXiv:2010.11929*, 2020. 5
- [15] R. Durall, M. Keuper, F.-J. Pfrendt, and J. Keuper. Unmasking deepfakes with simple features. *arXiv preprint arXiv:1911.00686*, 2019. 2
- [16] G. Fant, A. Kruckenberg, and L. Nord. Durational correlates of stress in swedish, french and english. *Journal of phonetics*, 19(3-4):351–365, 1991. 7
- [17] W. Guan, W. Wang, J. Dong, B. Peng, and T. Tan. Collaborative feature learning for fine-grained facial forgery detection and segmentation. *arXiv preprint arXiv:2304.08078*, 2023. 2
- [18] A. Jain, N. Memon, and J. Togelius. A dataless faceswap detection approach using synthetic images. In *2022 IEEE International Joint Conference on Biometrics (IJCB)*, pages 1–7. IEEE, 2022. 2
- [19] T. Karras, S. Laine, and T. Aila. A style-based generator architecture for generative adversarial networks. In *Proceedings of the IEEE/CVF conference on computer vision and pattern recognition*, pages 4401–4410, 2019. 2
- [20] M. Kim, S. Tariq, and S. S. Woo. Fretal: Generalizing deepfake detection using knowledge distillation and representation learning. In *Proceedings*



- of the *IEEE/CVF conference on computer vision and pattern recognition*, pages 1001–1012, 2021. 2
- [21] D. E. King. Dlib-ml: A machine learning toolkit. *The Journal of Machine Learning Research*, 10:1755–1758, 2009. 5
- [22] P. Korshunov and S. Marcel. Deepfakes: a new threat to face recognition? assessment and detection. *arXiv preprint arXiv:1812.08685*, 2018. 2
- [23] P. Korshunov and S. Marcel. Improving generalization of deepfake detection with data farming and few-shot learning. *IEEE Transactions on Biometrics, Behavior, and Identity Science*, 4(3):386–397, 2022. 2
- [24] M. Kowalski. Faceswap. <https://github.com/MarekKowalski/FaceSwap>. Accessed: 2023-02-16. 5
- [25] L. Li, J. Bao, H. Yang, D. Chen, and F. Wen. Faceshifter: Towards high fidelity and occlusion aware face swapping. *arXiv preprint arXiv:1912.13457*, 2019. 2, 5
- [26] L. Li, J. Bao, T. Zhang, H. Yang, D. Chen, F. Wen, and B. Guo. Face x-ray for more general face forgery detection. In *Proceedings of the IEEE/CVF conference on computer vision and pattern recognition*, pages 5001–5010, 2020. 2, 7
- [27] X. Li, Y. Lang, Y. Chen, X. Mao, Y. He, S. Wang, H. Xue, and Q. Lu. Sharp multiple instance learning for deepfake video detection. In *Proceedings of the 28th ACM international conference on multimedia*, pages 1864–1872, 2020. 7
- [28] Y. Li, M.-C. Chang, and S. Lyu. In ictu oculi: Exposing ai created fake videos by detecting eye blinking. In *2018 IEEE international workshop on information forensics and security (WIFS)*, pages 1–7. IEEE, 2018. 2
- [29] Y. Li, X. Yang, P. Sun, H. Qi, and S. Lyu. Celeb-df: A large-scale challenging dataset for deepfake forensics. In *Proceedings of the IEEE/CVF conference on computer vision and pattern recognition*, pages 3207–3216, 2020. 5
- [30] D. Lian, D. Zhou, J. Feng, and X. Wang. Scaling & shifting your features: A new baseline for efficient model tuning. *arXiv preprint arXiv:2210.08823*, 2022. 1, 3, 4
- [31] H. Liu, X. Li, W. Zhou, Y. Chen, Y. He, H. Xue, W. Zhang, and N. Yu. Spatial-phase shallow learning: rethinking face forgery detection in frequency domain. In *Proceedings of the IEEE/CVF conference on computer vision and pattern recognition*, pages 772–781, 2021. 7
- [32] Y. Luo, Y. Zhang, J. Yan, and W. Liu. Generalizing face forgery detection with high-frequency features. In *Proceedings of the IEEE/CVF conference on computer vision and pattern recognition*, pages 16317–16326, 2021. 7
- [33] I. Masi, A. Killekar, R. M. Mascarenhas, S. P. Gurudatt, and W. AbdAlmageed. Two-branch recurrent network for isolating deepfakes in videos. In *Computer Vision—ECCV 2020: 16th European Conference, Glasgow, UK, August 23–28, 2020, Proceedings, Part VII 16*, pages 667–684. Springer, 2020. 7
- [34] F. Matern, C. Riess, and M. Stamminger. Exploiting visual artifacts to expose deepfakes and face manipulations. In *2019 IEEE Winter Applications of Computer Vision Workshops (WACVW)*, pages 83–92. IEEE, 2019. 2
- [35] A. V. Nadimpalli and A. Rattani. On improving cross-dataset generalization of deepfake detectors. In *Proceedings of the IEEE/CVF Conference on Computer Vision and Pattern Recognition*, pages 91–99, 2022. 2
- [36] H. H. Nguyen, J. Yamagishi, and I. Echizen. Use of a capsule network to detect fake images and videos. *arXiv preprint arXiv:1910.12467*, 2019. 2
- [37] Y. Nitzan, K. Aberman, Q. He, O. Liba, M. Yarom, Y. Gandselman, I. Mosseri, Y. Pritch, and D. Cohen-Or. Mystyle: A personalized generative prior. *ACM Transactions on Graphics (TOG)*, 41(6):1–10, 2022. 2
- [38] I. Perov, D. Gao, N. Chervoniy, K. Liu, S. Marangonda, C. Umé, M. Dpfks, C. S. Facenheim, L. RP, J. Jiang, et al. Deepfacelab: Integrated, flexible and extensible face-swapping framework. *arXiv preprint arXiv:2005.05535*, 2020. 2, 4
- [39] Y. Qian, G. Yin, L. Sheng, Z. Chen, and J. Shao. Thinking in frequency: Face forgery detection by mining frequency-aware clues. In *Computer Vision—ECCV 2020: 16th European Conference, Glasgow, UK, August 23–28, 2020, Proceedings, Part XII*, pages 86–103. Springer, 2020. 7
- [40] M. A. Rahman and Y. Wang. Optimizing intersection-over-union in deep neural networks for image segmentation. In *International symposium on visual computing*, pages 234–244. Springer, 2016. 5
- [41] N. Rahmouni, V. Nozick, J. Yamagishi, and I. Echizen. Distinguishing computer graphics from natural images using convolution neural networks. In *2017 IEEE workshop on information forensics and security (WIFS)*, pages 1–6. IEEE, 2017. 2
- [42] H. Rezatofighi, N. Tsoi, J. Gwak, A. Sadeghian, I. Reid, and S. Savarese. Generalized intersection over union: A metric and a loss for bounding box regression. In *Proceedings of the IEEE/CVF conference on computer vision and pattern recognition*, pages 658–666, 2019. 5
- [43] R. Rombach, A. Blattmann, D. Lorenz, P. Esser, and B. Ommer. High-resolution image synthesis with latent diffusion models. In *Proceedings of the IEEE/CVF Conference on Computer Vision and Pattern Recognition*, pages 10684–10695, 2022. 1, 2
- [44] A. Rössler, D. Cozzolino, L. Verdoliva, C. Riess, J. Thies, and M. Nießner. FaceForensics++: Learning to detect manipulated facial images. In *International Conference on Computer Vision (ICCV)*, 2019. 4, 5, 7
- [45] S. Saha and T. Sim. Is face recognition safe from realizable attacks? In *2020 IEEE International Joint Conference on Biometrics (IJCB)*, pages 1–8, 2020. 2
- [46] M. Sharif, S. Bhagavatula, L. Bauer, and M. K. Reiter. Accessorize to a crime: Real and stealthy attacks on state-of-the-art face recognition. In *Proceedings of the 2016 ACM SIGSAC conference on computer and communications security*, pages 1528–1540, 2016. 2
- [47] Z. Sun, Y. Han, Z. Hua, N. Ruan, and W. Jia. Improving the efficiency and robustness of deepfakes detection through precise geometric features. In *Proceedings of the IEEE/CVF Conference on Computer Vision and Pattern Recognition*, pages 3609–3618, 2021. 2
- [48] J. Thies, M. Zollhöfer, and M. Nießner. Deferred neural rendering: Image synthesis using neural textures. *ACM Transactions on Graphics (TOG)*, 38(4):1–12, 2019. 2, 5
- [49] J. Thies, M. Zollhöfer, and M. Nießner. Deferred neural rendering: Image synthesis using neural textures. *ACM Transactions on Graphics (TOG)*, 38(4):1–12, 2019. 4
- [50] J. Thies, M. Zollhofer, M. Stamminger, C. Theobalt, and M. Nießner. Face2face: Real-time face capture and reenactment of rgb videos. In *Proceedings of the IEEE conference on computer vision and pattern recognition*, pages 2387–2395, 2016. 2, 5
- [51] R. Tzaban, R. Mokady, R. Gal, A. Bermano, and D. Cohen-Or. Stitch it in time: Gan-based facial editing of real videos. In *SIGGRAPH Asia 2022 Conference Papers*, pages 1–9, 2022. 2
- [52] A. Vaswani, N. Shazeer, N. Parmar, J. Uszkoreit, L. Jones, A. N. Gomez, Ł. Kaiser, and I. Polosukhin. Attention is all you need. *Advances in neural information processing systems*, 30, 2017. 2, 4
- [53] Y. Xu, K. Raja, L. Verdoliva, and M. Pedersen. Learning pairwise interaction for generalizable deepfake detection. In *Proceedings of the IEEE/CVF Winter Conference on Applications of Computer Vision*, pages 672–682, 2023. 2
- [54] X. Yang, Y. Li, and S. Lyu. Exposing deep fakes using inconsistent head poses. In *ICASSP 2019-2019 IEEE International Conference on Acoustics, Speech and Signal Processing (ICASSP)*, pages 8261–8265. IEEE, 2019. 2
- [55] H. Zhao, W. Zhou, D. Chen, T. Wei, W. Zhang, and N. Yu. Multi-attentional deepfake detection. In *Proceedings of the IEEE/CVF conference on computer vision and pattern recognition*, pages 2185–2194, 2021. 2, 7
- [56] J.-Y. Zhu, T. Park, P. Isola, and A. A. Efros. Unpaired image-to-image translation using cycle-consistent adversarial networks, 2017. 2
- [57] B. Zi, M. Chang, J. Chen, X. Ma, and Y.-G. Jiang. Wilddeepfake: A challenging real-world dataset for deepfake detection. In *Proceedings of the 28th ACM international conference on multimedia*, pages 2382–2390, 2020. 5